Applied Surface Science 656 (2024) 159703

Contents lists available at ScienceDirect

Applied Surface Science

journal homepage: www.elsevier.com/locate/apsusc

Full Length Article

X-ray induced degradation during XPS analysis of dicarboxylic acid powders

José Mario Ferreira Jr [a,1,*], Gustavo F. Trindade [b,c,1], George Simonelli [d], Carlos Augusto de Morais Pires [d], Ana Cristina Morais da Silva [d], Jesualdo Luiz Rossi [e], Luiz Carlos Lobato dos Santos [d], Patrick Alfred Johnson [a,1,*]

[a] Department of Materials Science and Engineering, Iowa State University, Ames, IA 50011, USA
[b] Faculty of Engineering and Physical Sciences, University of Surrey, Surrey GU2 7XH, UK
[c] National Physical Laboratory, Teddington TW11 0LW, UK
[d] Chemical Engineering Postgraduate Program, Federal University of Bahia, 40210-630, Brazil
[e] Nuclear and Energy Research Institute - IPEN, São Paulo 05508-000, Brazil

ARTICLE INFO

Keywords:
XPS
Dicarboxylic acids
Malonic acid
Succinic acid
Glutaric acid
Thermal decomposition
Surface analysis

ABSTRACT

It is widely recognized that exposure to X-rays during XPS analysis can decompose different materials, resulting in mass loss and changes in chemical composition. These effects are evident in the near-edge X-ray absorption structure spectra of dicarboxylic acid powders, posing a fundamental limit to sensitivity for surface chemical analysis. Understanding the chemistry and kinetics of radiation decomposition is necessary for the accuracy and validation of XPS analysis on dicarboxylic acids. Here we evaluate the impact of X-ray exposure on characterizing chemical changes in three different dicarboxylic acids with varying aliphatic carbon chain lengths. From this investigation we propose straightforward correlations relating the tendency for radiation-induced decomposition based on the chemical structure of the acids. We employed two types of spectra, those acquired with minimal interaction (snapshot) and high-resolution spectra obtained over an extended period, to show that normal analysis conditions are likely to degrade these type of materials.

1. Introduction

X-ray photoelectron spectroscopy (XPS) is performed by irradiating a material with an X-ray beam while measuring the kinetic energy and the number of electrons emerging from the top 0 to 12 nm of the material [1–4]. The primary radiation source for X-ray photoelectron spectroscopy is soft X-rays, usually AlKα [1–6]. Due to the versatility of different materials that can be analyzed and the relatively simple configuration of the analysis preparation, many studies neglect the stability of analyzed species (organic and inorganic) under X-ray radiation, which poses a risk to the accuracy of XPS analysis when decomposition caused during the analysis is significant and presents results referring to the decomposition products rather than the chemical state of the actual material [1–8].

Linear saturated dicarboxylic acids have carboxyl functional groups (–COOH) at the extremities of their aliphatic chains and can be represented by the general molecular formula HOOC–(CH2)n-COOH. These acids are widely used as precursors in the production of copolymers, catalysts, corrosion resistance coatings and additives for electrodeposition of protective coatings [9,10]. The understanding of the extent of the decomposition generated by X-rays and the kinetics correlated to this decomposition allows the adoption of experimental work procedures close to a tolerable decomposition limit. Often, the XPS analysis procedures for carboxylic acids, dicarboxylic acids, and their salts (carboxylates and dicarboxylates) are performed without evidence of concern for the effects of the X-rays and without reporting decomposition in the obtained data [11–17]. Moreover, the concern with radiation decomposition during XPS analysis increases with the need for higher spatial resolution with more focused X-rays beams. Comprehensive work has been done to try to address and understand degradation of polymers during XPS analysis and defects caused by prolonged irradiation [18–23].

We previously published a series of reference spectra for dicarboxylic

* Corresponding authors.
E-mail addresses: josemf1@iastate.edu (J.M. Ferreira Jr), paj3@iastate.edu (P.A. Johnson).
[1] These authors contributed equally to this work.

https://doi.org/10.1016/j.apsusc.2024.159703
Received 9 October 2023; Received in revised form 9 February 2024; Accepted 12 February 2024
Available online 14 February 2024

acids where two systematic degradation products were observed for the carbon peak (**DP1** 286.8 eV and **DP2** 290.5 eV) and one peak for oxygen (**DP2*** 534.1 eV) [9,10]. The decomposition of carboxylic groups by radiation can take various forms, such as loss of crystallinity, loss of mass, or chemical modification. The present study is focused on the XPS induced chemical modifications manifested in spectral changes. The results enable better understanding of the decomposition of dicarboxylic acids under X-ray radiation during XPS analyses, and also highlight good practices for the acquisition of accurate XPS spectra from samples of X-ray sensitive powders. A series of dicarboxylic acids have been examined: propanedioic acid (malonic acid), butanedioic acid (succinic acid), and pentanedioic acid (glutaric acid). The induced chemical changes of these dicarboxylic acids were examined by comparing the XPS spectra acquired with minimal X-ray interaction ("snapshots") and different exposure levels (through the continuous acquisition of high-resolution C 1 s and O 1 s spectra).

2. Methodology

2.1. Sample preparation

Dicarboxylic acid powders: malonic acid ($C_3O_4H_4$), succinic acid ($C_4O_4H_6$), and glutaric acid ($C_5O_4H_8$), with 99 % purity were obtained from Sigma®. A small amount of powder was placed in the XPS sample port, manually pressed, and analyzed. For each of the dicarboxylic acids studied, five samples were prepared and used in specific experimental conditions. Three analysis points in a straight line corresponding to the diameter of the sample holder (left, center and right point) were used in all analyses. For each of these three points, a "snapshot" spectrum for C 1 s (285 eV) was acquired to ensure homogeneity and reproducibility. Concentration deviations greater than 1 % between these points resulted in sample discard.

2.2. XPS analyses

All XPS measurements were performed with a Theta Probe system from Thermo Fisher Scientific, UK. For control and data acquisition as well for the data evaluation, the *Avantage* software package provided by the system manufacturer was used. The high-resolution XPS spectra were acquired with the following parameters: monochromatic AlKα X-ray gun radiation source (1486.7 eV), 16 kV voltage, 6.3 mA emission current, 400 μm spot size, 50 eV pass energy, 0.2 eV energy channels, and pressure of the analysis chamber in the 10^{-9} mbar range. Charge neutralization on the sample surface was obtained via a standard dual flood gun, which provides electrons of low energy (typically −2 eV). During application of the flood gun, the chamber pressure was in the lower half of the 10^{-7} mbar range. Total time for a single spectrum was 101 s.

The XPS snapshot spectra were used as reference for "undegraded" signal and acquisition parameters were the same for carbon and oxygen mentioned above. The time to acquire a single spectrum was limited to 1 s. For data analysis, the background was eliminated by applying Shirley background subtraction and the peak-areas normalized using Scofield sensitivity factors to obtain the elemental composition of the surface.

To avoid cross-contamination between different samples, only one sample was mounted on a 1 cm^2 sample holder. In order to guarantee that the different technical repeats and areas were compatible, a quick check with a 1 s snapshot of the C 1 s peak was performed in a neighboring area before each measurement. Each of the dicarboxylic acids, now divided into five samples, were used for the acquisition of: (a) survey spectra; (b) C 1 s snapshot; (c) O 1 s snapshot; (d) C 1 s high-resolution spectra, and (e) O 1 s high-resolution spectra. The X-ray incidence times in the XPS analyzes listed were respectively, survey spectrum (3 scans) corresponding to 510 s, C 1 s and O 1 s snapshot (1 scan) corresponding to 1 s each, C 1 s high-resolution spectra and O 1 s high-resolution spectra (varying from 20 to 1600 scans or 101 s to 8080 s). The results presented are the average of two values obtained from two different locations of the analyte and with a deviation of less than 1 %. Charge shift compensation with C-C set to 284.8 eV was necessary for this study since absolute binding energy values were of concern for data evaluation. The values used in the charge compensation will be presented individually, referring to each spectrum (snapshot and high-resolution spectrum).

The chemical structures of the dicarboxylic acids with the elements identified are shown in Fig. 1. The carbons of the dicarboxylic acid chains are designated as A, B and C corresponding respectively to the β carbon, carboxylic groups, and aliphatic carbon. The oxygen in the carbonyl group and the hydroxyl group oxygen were designated as c and d respectively.

For some molecules, the peak positions are reported for a peak fit to the spectrum, which includes a separate peak for the backbone carbon that is directly bonded to the carboxyl carbon. This carbon has been assigned to a different binding energy BE than other hydrocarbon species because of the next-nearest-neighbor effect induced by the carboxyl oxygens (-0.7 eV BE shift). The inclusion of a separate peak for this 'beta-shifted' induced carbon environment has been justified previously for several types of polymers and molecules [23–32]. It is difficult to differentiate between the C-C/C-H carbons and the 'beta-shifted' carbon and attempts to do so can introduce significant errors in analysis. Therefore, the results in this work report the sum of these carbons at position 285 eV.

3. Results and discussion

3.1. Identification of degradation products

Based on the molecular structure of the acids studied we can predict the expected binding energies of the various carbon species and the associated oxygen species. These include the aliphatic carbon bonds (C-C/C-H at 285.0), the beta-shifted carbon (HOOC-C* at 285.0 eV), the carboxylate carbon (289.0 eV), as well as the O1s binding energies from the carboxyl group, (C = O at 532.0 eV and OH at 533.2 eV). An ideal spectrum should have only these peaks at their correct proportions as shown in the theoretical spectra represented in Fig. 2.

From the chemical structures and the expected binding energy states of carbon for the dicarboxylic acids, the relative ratios of C-C/C-H + Carbon β to COOH for malonic acid (1/2), succinic acid (2/2), and glutaric acid (3/2) can be predicted. When differentiating the two different oxygen states, independent of the analyzed acid dicarboxylic, the expected quantities are equal (1/1). Table 1 shows the relative concentrations of carbon and oxygen in atomic percentages.

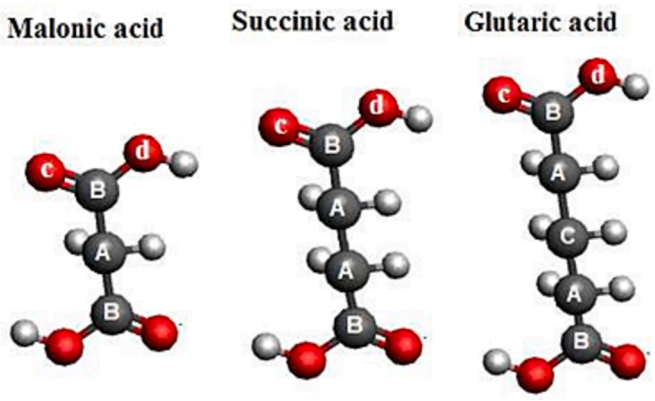

Fig. 1. Chemical structures of dicarboxylic acids (malonic, succinic and glutaric) with carbons and oxygens (A - carbon β, B - functional carbon (carboxylic group), C - aliphatic carbon, c - oxygen from carbonyl, and d - oxygen from hydroxyl group) [8,9].

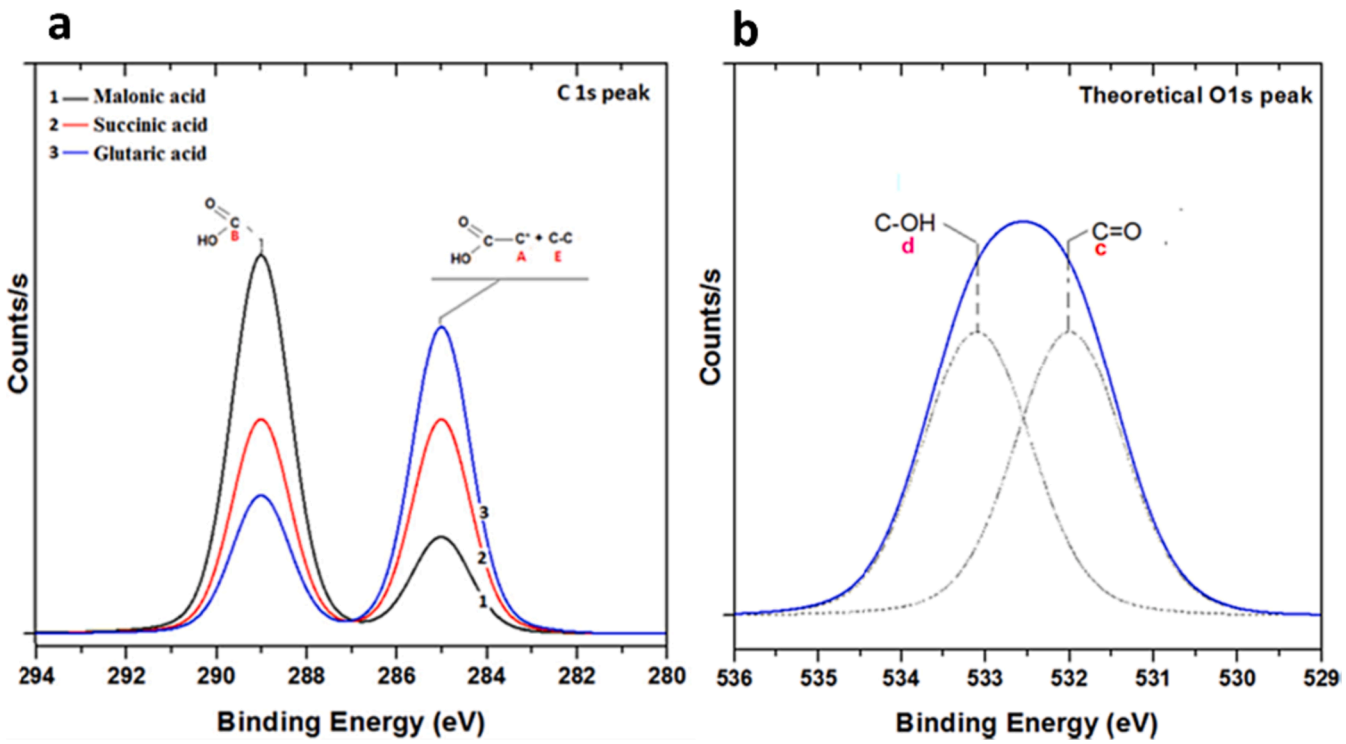

Fig. 2. Theoretical XPS Peaks of malonic, succinic, and glutaric carboxylic diacids: (a) carbon (C 1 s), A - carbon β + C-C/C-H, and B - COOH, and (b) oxygen (O 1 s), c - HO-C, and d - O = C [8].

Table 1
Expected ratios between the elements in atomic concentration for malonic, succinic, and glutaric acids.

Acid	C/total	O/total	COOH/Ctotal	C-C/COOH
Malonic	3/7 (42.85)	4/7 (57.15)	2/3 (66.66)	1/2
Succinic	4/8 (50.00)	4/8 (50.00)	2/4 (50.00)	2/2
Glutaric	5/9 (55.55)	4/9 (44.45)	2/5 (40.00)	3/2

Fig. 3a–c and Fig. 4a–c present snapshot spectra for carbon and oxygen for the malonic, succinic, and glutaric acids. The XPS snapshot spectra for carbon and oxygen showed that the peak fitting was done with minimum deviation and with only two fitted peaks for both elements. The information obtained on the carbon and oxygen fittings for the dicarboxylic acids is presented in Table 2. The results show that the snapshot spectra do not present a large deviation from the theoretical values. However, snapshot spectra are not commonly used as a quantitative method. These results clearly illustrate the importance of obtaining snapshot spectra for a comparative base in case any degradation is being induced by X-rays irradiation. It is important to note that for all samples the carbon content is higher than the theoretical values for malonic (3.0 %), succinic (3.8 %) and glutaric acids (4.3 %). The carbon content increase in powder samples is often attributed to atmospheric CO_2 contamination via adsorption [33–37].

Fig. 3d–f and Fig. 4d-f show the carbon and oxygen spectra with fitted peaks for the malonic, succinic, and glutaric acids acquired after 101 s (20 scans). The standard way of analysis is to acquire survey spectrum followed by high-resolution spectrum at the same point of a detected species. When multiple high-resolution spectra are acquired at the same point, the degradation will accumulate and be more significant. Based on this, a survey spectra acquisition time (505 s) was added to the acquisition time of 20 scans for carbon (101 s), equaling 606 s of irradiation at a single point. Fig. 3g–I and Fig. 4g-i show the carbon and oxygen spectra after 606 s of irradiation.

The results show that 101 s of X-ray incidence is enough to change the spectra in relation to snapshot spectra with two new fitted peaks for carbon (DP_1 286.8 eV and DP_2 290.5 eV) and one component for Oxygen (DP_{2*} 534.1 eV). This indicates that XPS data of dicarboxylic acids can be misleading with results presenting a stage of degradation rather than their real (original) chemical states. The degradation is noted after approximately one fifth of the time required to acquire a Survey spectrum (510 s), which is usually taken as the first analysis.

The fact that the central C atom in each case has a higher concentration of oxygen in its environment suggests that the DP1 peak may be C-O (typically located at 286.5 eV) [23–32]. The DP2* peak, on the other hand, has a higher binding energy than C-OH, suggesting oxygen in an environment where there is less electron donation to the O than in C-O. Therefore, the origin of DP2* is correlated with the appearance of the DP1 and DP2 peaks. This DP2* peak is indicative of oxygen singly bound to carbon in the C-OH bond, as well as chemisorbed oxygen (1 s → π*) and/or water (chemisorbed H_2O/C-OH)) [23–32]. The second CO_2 species present on both surfaces is physiosorbed CO_2 exhibiting an O 1 s BE of 534.5 eV. This species is attributed to trapped CO_2 molecules. The adsorption of CO_2 induces the coalescence of the chains and thus traps the CO_2. Surface carbonates and physiosorbed CO_2 are typically found in XPS at BEs between 289 and 293 eV [33–37]. Thus, according to the BE position of this peak, it is assigned to CO_2 species resulting from decarboxylation because of α-C-COOH bond scission. The information obtained from the carbon and oxygen fitting peaks to dicarboxylic acids is summarized in Table 2.

Significantly, prolonged time of irradiation led to a major change in the concentrations of the COOH groups. For all dicarboxylic acids

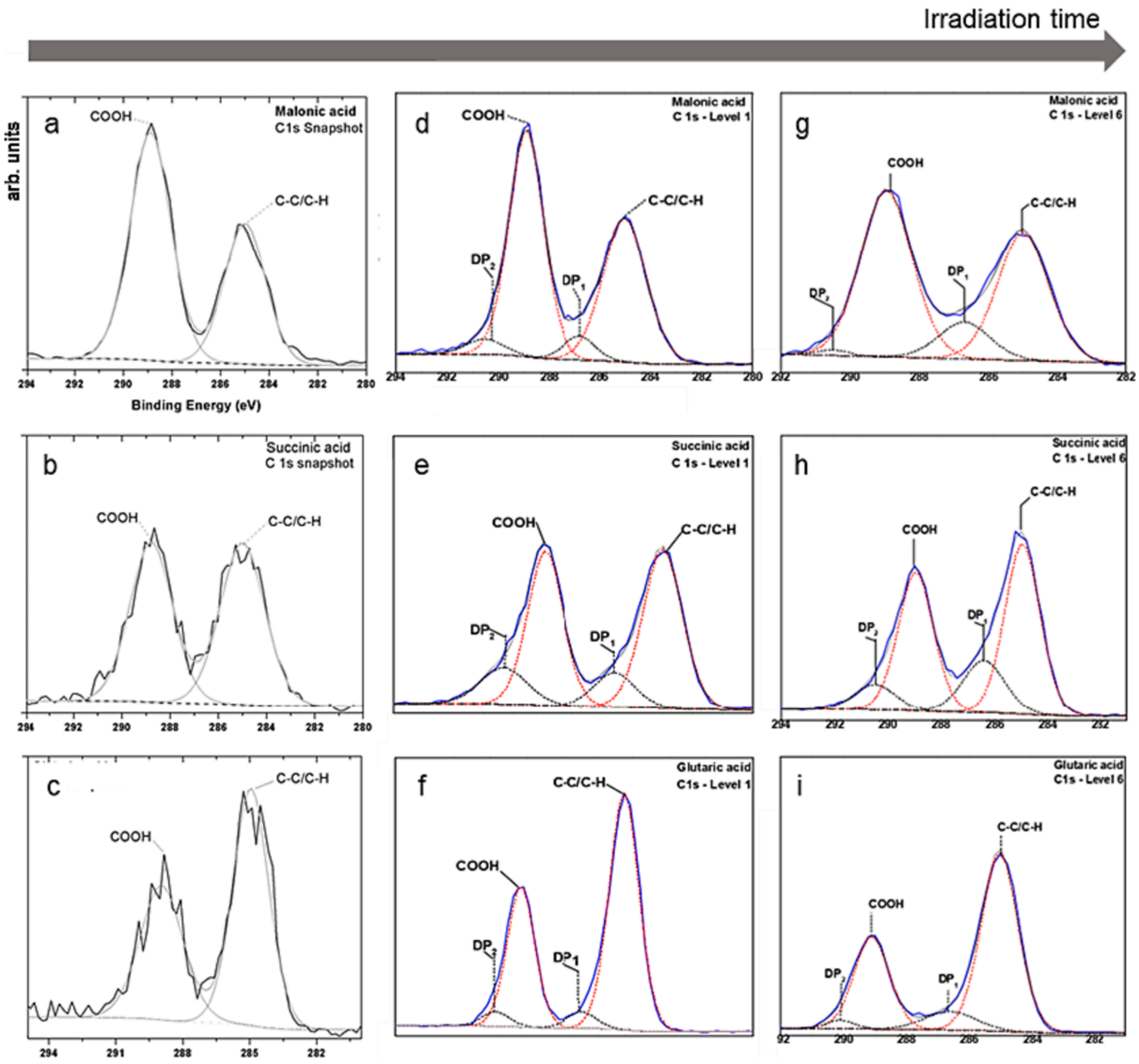

Fig. 3. XPS C1s snapshot(a-c) and high-resolution spectra with fitted peaks for the malonic, succinic, and glutaric acids acquired after 101 s (d-f) and 606 s (g-i).

studied, the decarboxylation causes a decrease in the relative carbon values correspondent to the ratio between carboxylic group and the total number of carbons (COOH/Ctotal). For malonic acid degraded into acid ethanoic, this value goes from 2/3 to 1/2, to succinic acid degraded into propanoic acid, 2/4 to 1/3, and for glutaric acid degraded into butanoic acid, 2/5 to 1/4.

The proximity of these values to the theoretical values for the ethanoic, propanoic and butanoic monoacids show the advanced stage of degradation caused by the XPS analysis time. During irradiation, two effects are expected and are responsible for chemical changes, interaction of radiation with the organic acid and the thermal effect resulting from this interaction. In this work, only the portion referring to the thermal effect as an agent for changing chemical states is considered. In general, studies on thermal analyses of dicarboxylic acids report the decomposition to form monocarboxylic acid by decarboxylation, describing different numbers of steps and products for the formation of a lower monocarboxylic acid chain. The thermal decomposition of dicarboxylic acids is described by the formation of a monoacid with one carbon less than the initial dicarboxylic acid, formed by the loss of a carboxylic functional group or by the formation and release of CO_2 [13–17], which is shown in the equations (1), 2 and 3 in simplified form [16,17].

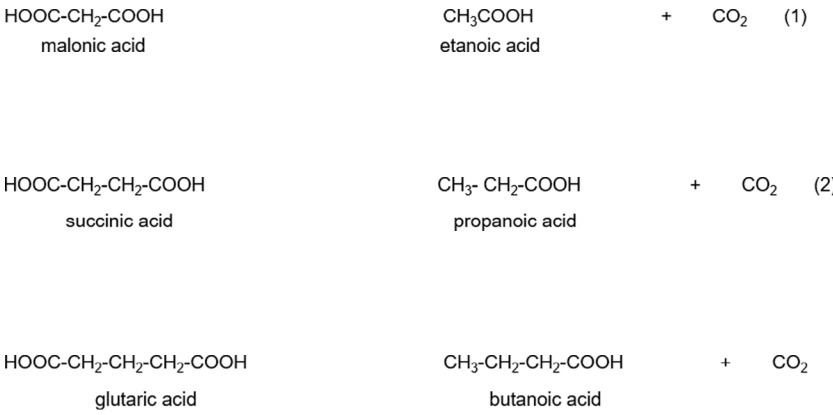

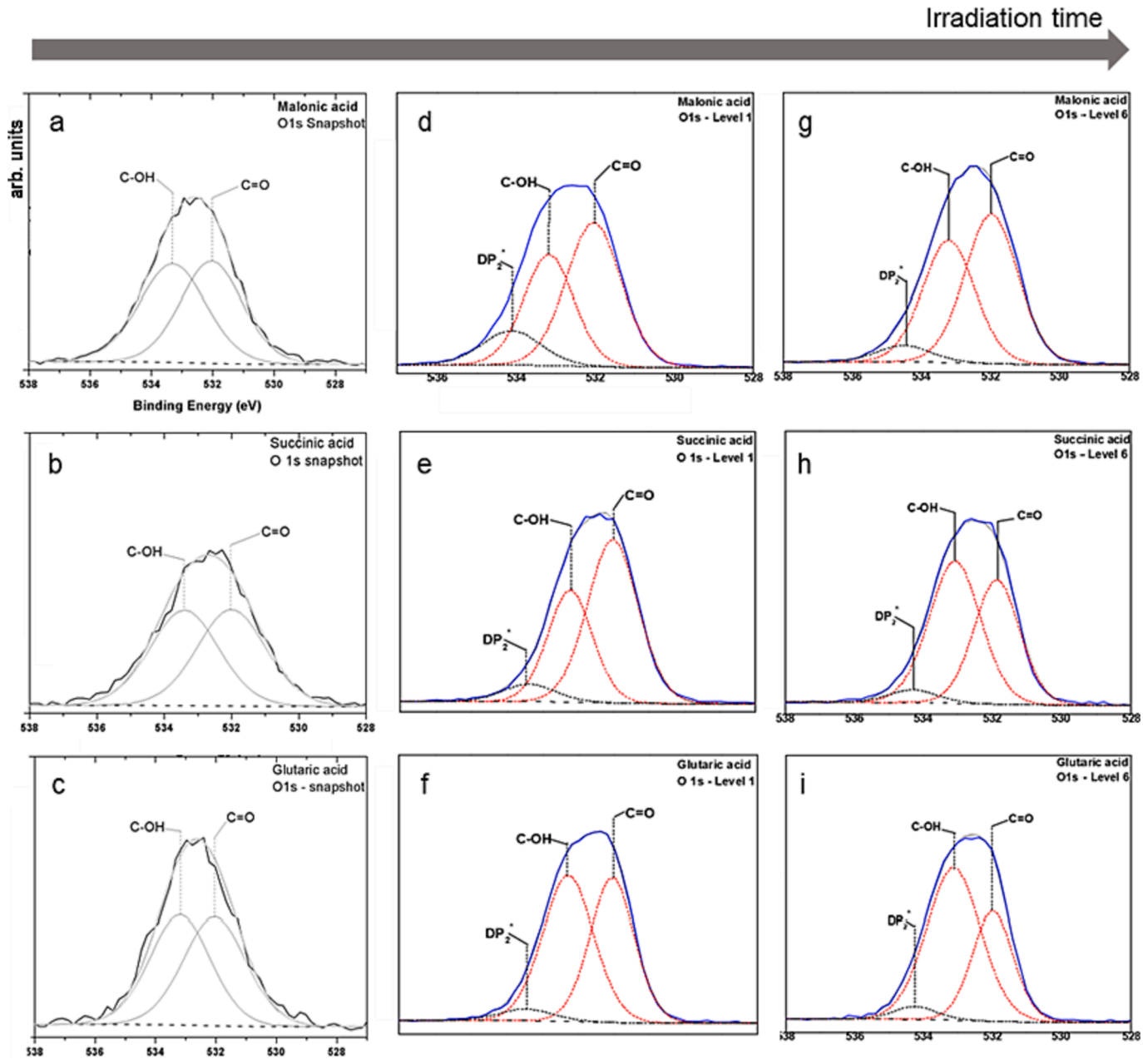

Fig. 4. XPS O1s snapshot(a-c) and high-resolution spectra with fitted peaks for the malonic, succinic, and glutaric acids acquired after 101 s (d-f) and 606 s (g-i).

Table 2
Peak designation, binding energy, FWHM, atomic concentration, and deviation obtained from high- resolution spectra peak fitting of carbon, and oxygen peaks.

			Theoretical	Snapshot			101 s (20 scans)			606 s (Survey + 20 scans)		
Sample		Peak designation	At. %	Peak BE (eV)	FWHM eV	At.%	Peak BE (eV)	FWHM eV	At.%	Peak BE (eV)	FWHM eV	At.%
		C 1s	42.9	288.9	1.6	45.8	288.9	1.6	44.5	288.9	1.6	44.5
		O 1s	57.1	532.6	2.6	54.2	532.4	2.6	55.5	532.4	2.6	55.5
		C-C/C-H	33.3	285.0	2.0	38.2	285.0	1.7	40.1	285.0	1.7	38.3
Malonic acid	C 1s	DP_1	0.0	-	-	0.0	286.8	1.5	5.0	286.7	1.7	10.9
		COOH	66.7	288.9	2.0	61.8	288.9	1.6	51.3	288.9	1.7	49.8
		DP_2	0.0	-	-	0.0	290.5	1.7	3.7	290.5	1.0	1.0
		O=C	50.0	532.0	2.4	49.1	532.0	1.6	51,00	532.0	1.9	52.1
	O 1s	HO-C	50.0	533.3	2.6	50.9	533.2	1.5	35.9	533.3	1.9	42.0
Charge shift +0.93 eV		DP_{2^*}	0.0	-	-	0.0	534.1	1.8	13.1	534.5	1.9	5.9
		C 1s	50.0	289.0	1.7	53.8	289.0	1.7	53.3	289.0	1.7	53.3
		O 1s	50.0	532.7	2.6	46.2	532.6	2.6	46.7	532.6	2.6	46.7
		C-C/C-H	50.0	285.0	2.2	51.4	285.0	1.5	41.9	285.0	1.6	42.4
	C 1s	DP_1	0.0	-	-	0.0	286.6	1.6	9.5	286.4	1.9	15.7
Succinic acid		COOH	50.0	288.8	2.1	48.6	288.9	1.4	37.0	288.9	1.6	34.5
		DP_2	0.0	-	-	0.0	290.3	1.8	11.6	290.5	1.8	7.4
		O=C	50.0	532.0	2.4	50.3	532.0	1.7	58.3	532.0	1.7	41.8
	O 1s	HO-C	50.0	533.4	2.4	49.7	533.2	1.5	35.2	533.2	1.5	53.7
Charge shift +1.2 eV		DP_{2^*}	0.0	-	-	0.0	534.4	1.7	6.5	534.4	1.6	4.5
		C 1s	55.5	285.0	1.4	59.8	285.0	1.4	60.0	285.0	1.5	62.6
		O 1s	44.5	532.6	2.6	40.2	532.6	2.6	40.0	532.6	2.6	37.5
		C-C/C-H	60.0	285.0	2.0	60.1	285.0	1.4	59.5	285.0	1.4	59.8
Glutaric acid	C 1s	DP_1	0.0	-	-	0.0	286.7	1.4	4.2	286.6	1.9	8.7
		COOH	40.0	289.0	2.4	39.9	289.1	1.3	32.9	289.1	1.3	29.5
		DP_2	0.0	-	-	0.0	290.1	1.3	3.4	290.1	1.0	2.1
		O=C	50.0	532.0	2.4	50.3	532.0	1.5	44.2	532.0	1.4	33.8
	O 1s	HO-C	50.0	533.1	2.4	49.7	533.3	1.7	51.5	533.1	1.8	62.0
Charge shift +1.6 eV		DP2*	0.0	-	-	0.0	534.5	1.7	4.3	534.2	1.5	4.19

The reported values of the melting point for malonic, succinic and glutaric acids vary according to different authors and according to different environments used, but there is a consensus that the melting point is the reference point for the decomposition of these acids. The temperature values reported for forming the respective carboxylic acid from the thermal decomposition of dicarboxylic acids in inert atmosphere (Ar) were: 138 °C for malonic, 188 °C for succinic, and 100 °C for glutaric. Even though there is not a clear consensus on these temperatures, they will be used as a reference for a decomposition point [38,39].

3.2. Longer acquisition times to enable insights on degradation mechanisms

The acids studied here were chosen for having even numbered carbonic compounds (succinic acid) and odd chains (malonic and glutaric acids). It is assumed that the different temperature values for the formation of carboxylic acids from the thermal decomposition of even and odd carbon chain dicarboxylic acids are derived from interactions of the terminal groups with intermolecular hydrogen bonds. These interactions are more intense in even-chain dicarboxylic acids than for odd-chain dicarboxylic acids [38–41].

In part, the difference in the thermal decompositions of dicarboxylic acids is also associated with different crystalline structures, where malonic acid belongs to the triclinic system, and succinic and glutaric acids belong to the monoclinic system. The simplified form of decarboxylation shown in the previous equations is so named because pyrolysis work on these acids as well as thermal decomposition work show a more complex mechanism, often with the formation of anhydrates decomposed at higher temperatures than the current temperatures reported for the decarboxylation in a single step [40–42].

Cruz-Castañeda et al. report in their radiolysis experiment the thermal decomposition of malonic acid solutions, results showing the relative stability of malonic acid at temperatures of approximately 90—100 ^{0}C. At elevated temperatures, synthesis of potential biologically relevant molecules can occur, for example formation of acetic acid. Mechanisms for the formation of larger molecules by dimerization/condensation type reactions are also related [37]. According to these mechanisms, the temperatures for the formation of carboxylic acids are much higher than the temperatures reported for single-step degradation, so further measurements were carried out for longer periods of time to enable insights on the type of mechanism associated with the degradation of the carboxylic acids during X-ray irradiation. The XPS spectra for carbon and oxygen were obtained for up to 8080 s. Results are shown in Fig. 5.

The results show an increase in the relative concentration of carbon for all acids. A decrease in the same ratio of the values of the atomic concentration of oxygen is observed. This behavior is due to the decarboxylation of dicarboxylic acids, in which the loss of a carboxylic group represents a loss of one carbon and two oxygens. For malonic acid the atomic concentration of carbon and oxygen is equal (50 % each) at 1010 s of X-Ray incidence (equation (1), showing that this analysis time is enough for its decomposition forming ethanoic acid.

The succinic and glutaric acids had their equivalent decompositions at 1363 s and 2525 s, respectively. with atomic concentrations of carbon corresponding to propanoic and butanoic acids (Equations (2) and (3). A more accurate view of the events during XPS analysis over an extended

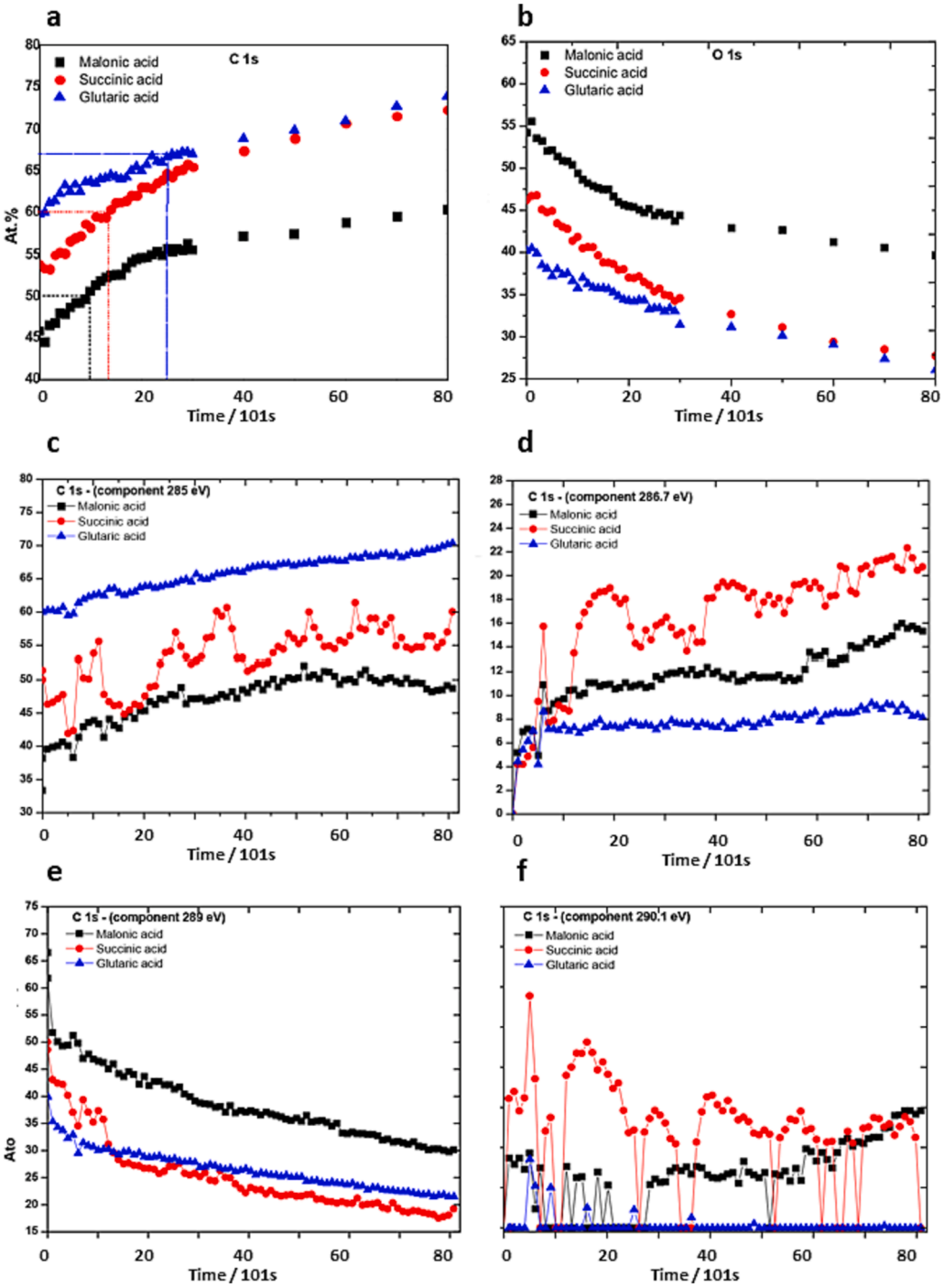

Fig. 5. The atomic concentration of total carbon (a) and total oxygen (b) for malonic, succinic, and glutaric acids as a function of XPS analysis time. Fitted carbon spectra peaks at (a) 285 eV (C-C/C-H), (b) 286.7 eV (DP1-CO), (c) 289 eV (–COOH) and (d) 290.1 eV (DP2-CO2 adsorbed) as a function of XPS analysis time.

time can be observed when analyzing individual components of the C1s spectra at 285 eV (CC/C-H), 286.7 eV (DP_1-CO), 289 eV (–COOH) e 290.1 eV (DP_2-CO_2 adsorbed) (Fig. 5c–f).

The DP1-CO peak increases according to glutaric < malonic < succinic which suggests that decarboxylation is the final stage of decomposition. Similarly, the progressive decomposition is evidenced by the change in concentration of aliphatic carbon and the decrease in the relative carbons of the carboxylic group. For the succinic acid results, the oscillating values can be associated with the formation of chemical transition states (Fig. 5d, f).

The ratio between the concentrations of COOH and C-C (COOH / C-C) is an efficient parameter to define the X-ray incidence time by XPS analysis at which the degradations fully occurred, forming the decarboxylated products. This is because, theoretically, malonic acid forms ethanoic acid after undergoing decarboxylation with a COOH/C-H ratio = 1. After decarboxylation, succinic acid will form propanoic acid with a COOH/C-H ratio = 1/2 and finally the glutaric acid losing a carboxylic group and decomposing into butanoic acid with a COOH/C-H ratio = 1/3 (See Table 1). These ratios as a function of analysis time for succinic and glutaric malonic acids are shown in Fig. 6a.

The results show that for malonic acid, the ratio between the aliphatic carbon and carboxylate group is 1, corresponding to the

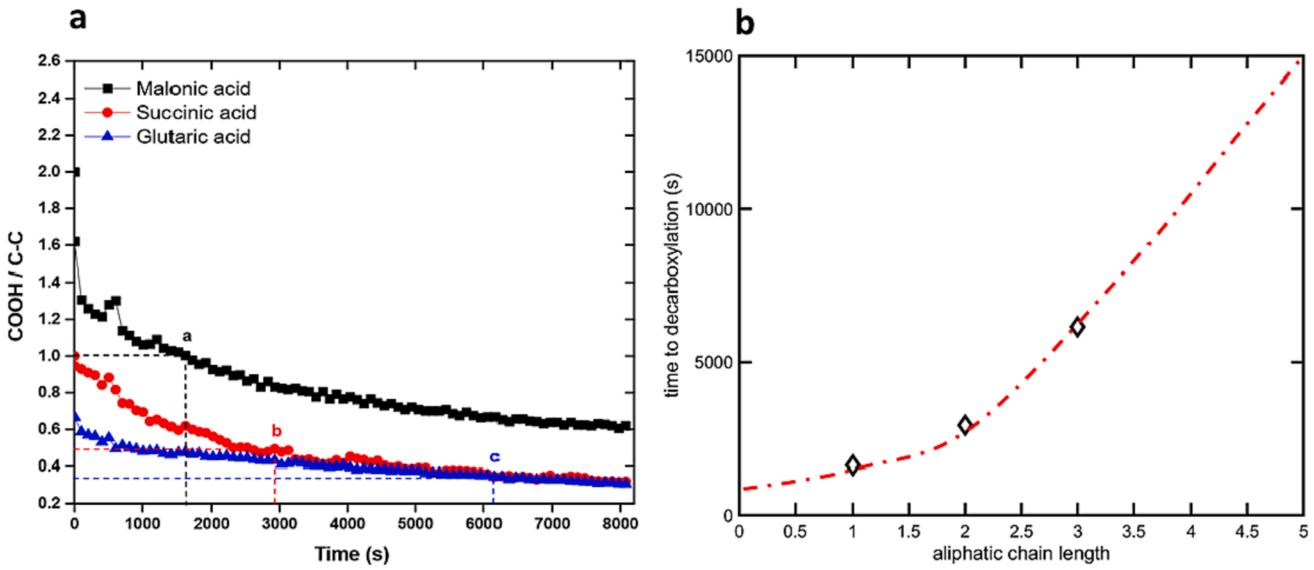

Fig. 6. (a) The atomic concentration ratio carboxylic groups and aliphatic carbons in function of analysis time. The correspondent points ratios COOH/C-H point a malonic acid ratio = 1, point b succinic acid ratio = 1/2 and point c glutaric acid ratio = 1/3. (b) Relationship between aliphatic chain length and time to decarboxylation.

formation of ethanoic acid after approximately 1630 s. Succinic acid has a COOH/C-H ratio equal to 1/2 corresponding to propanoic acid after approximately 2926 s. and glutaric acid, the COOH/C-H ratio is evident after 6163 s. It is worth remembering that the expected temperatures for the decarboxylation of these dicarboxylic acids are approximately 138 °C (malonic acid), 188 °C (succinic acid) and 100 °C (glutaric acid). These times show a dependency with the aliphatic chain length (and stability) of each acid (Fig. 6b).

4. Conclusion

We demonstrated that minimal interaction time between X-rays and dicarboxylic acid powders corresponding to typical XPS survey spectra acquisition is enough to cause degradation, resulting in spectra reflecting the degradation products as opposed to the initial molecules being studied. The most accurate analysis for dicarboxylic acids by XPS is the snapshot acquisition, a result obtained by the minimum possible interaction between sample and X-ray. The main hypothesis for our observations is that the interaction of X-rays with samples during analysis causes generation of heat that is responsible for the degradation of the analyte. Several effects were observed: a decrease in the intensity of specific spectral characteristics attributed to the loss of functional groups, and the observation of new spectral characteristics attributed to the formation of a new chemical structure. Analysis at different times of X-rays exposure allowed the determination of a critical time which should be useful for XPS practitioners to define adequate limits for analytical experiments. In future work we aim to generalize the approach and establish critical X-rays doses (or critical induced temperatures) that can be applied to any material with known thermal properties. Generally, XPS is not carried out for long periods (up to 8000 s) as adopted in this work, but this method has been useful to verify decomposition and validate the hypothesis of thermal degradation.

CRediT authorship contribution statement

José Mario Ferreira Jr: Writing – review & editing, Writing – original draft, Supervision, Project administration, Methodology, Investigation, Funding acquisition, Formal analysis, Data curation, Conceptualization. **Gustavo F. Trindade:** Software, Methodology, Formal analysis, Data curation. **George Simonelli:** Writing – review & editing, Visualization, Software, Methodology. **Carlos Augusto de Moraes Pires:** Writing – review & editing, Writing – original draft, Formal analysis, Conceptualization. **Ana Cristina Morais Da Silva:** . **Jesualdo Luiz Rossi:** Writing – review & editing, Writing – original draft, Methodology. **Luiz Carlos Lobato dos Santos:** . **Patrick Alfred Johnson:** .

Declaration of competing interest

The authors declare the following financial interests/personal relationships which may be considered as potential competing interests: Jose Mario Ferreira Junior reports financial support was provided by National Council for Scientific and Technological Development.

Data availability

Data will be made available on request.

Acknowledgments

The authors wish to thank CNPq (process 200490/2014-1), for financial support of this research. Special thanks to Mark Baker, Steven Hinder and Professor John Watts from the University of Surrey.

References

[1] G. Greczynski, L. Hultman, X-ray photoelectron spectroscopy: towards reliable binding energy referencing, Prog. Mater. Sci. 107 (2020) 100591, https://doi.org/10.1016/j.pmatsci.2019.100591.
[2] A.G. Shard, X-ray photoelectron spectroscopy, in: V.-.-D. Hodoroaba, W.E.S. Unger, A.G. Shard (Eds.), Charact, Nanoparticles, Elsevier, 2020, pp. 349–371, https://doi.org/10.1016/B978-0-12-814182-3.00019-5.
[3] Y. Nakayama, S. Kera, N. Ueno, Photoelectron spectroscopy on single crystals of organic semiconductors: experimental electronic band structure for optoelectronic properties, J. Mater. Chem. C 8 (27) (2020) 9090–9132, https://doi.org/10.1039/D0TC00891E.
[4] J.A. McLeod, L. Liu, Prospects for mitigating intrinsic organic decomposition in methylammonium lead triiodide perovskite, J. Phys. Chem. Lett. 9 (9) (2018) 2411–2417, https://doi.org/10.1021/acs.jpclett.8b00323.
[5] Y. Li, B. Li, X. Zhao, N. Tian, J. Zhang, Totally waterborne, nonfluorinated, mechanically robust, and self-healing superhydrophobic coatings for actual anti-icing, ACS Appl. Mater. Interfaces 10 (45) (2018) 39391–39399.
[6] O. Sublemontier, C. Nicolas, D. Aureau, M. Patanen, H. Kintz, X. Liu, C. Miron, X-ray photoelectron spectroscopy of isolated nanoparticles, J. Phys. Chem. Lett. 5 (19) (2014) 3399–3403, https://doi.org/10.1021/jz501532c.
[7] P. Van der Heide, X-ray photoelectron spectroscopy: an introduction to principles and practices, John Wiley & Sons, Hoboken, 2011.

[8] J.F. Watts, J. Wolstenholme, An introduction to surface analysis by XPS and AES, John Wiley & Sons, Chichester, 2019.
[9] J.M. Ferreira, G.F. Trindade, R. Tshulu, J.F. Watts, M.A. Baker, Introduction to a series of dicarboxylic acids analyzed by x-ray photoelectron spectroscopy, Surf. Sci. Spectra 24 (1) (2017), https://doi.org/10.1116/1.4983448.
[10] G.F. Trindade, J.M. Ferreira, M.L. Abel, M.A. Baker, J.F. Watts, Dicarboxylic acids analyzed by time-of-flight secondary ion mass spectrometry. part 0: ethanedioic acid, Surf. Sci. Spectra 24 (2) (2017), https://doi.org/10.1116/1.5004981.
[11] A. Turco, M. Moglianetti, S. Corvaglia, S. Rella, T. Catelani, R. Marotta, P. P. Pompa, Sputtering-enabled intracellular X-ray photoelectron spectroscopy: a versatile method to analyze the biological fate of metal nanoparticles, ACS Nano 12 (8) (2018) 7731–7740, https://doi.org/10.1021/acsnano.8b01612.
[12] H. Ade, H. Stoll, Near-edge X-ray absorption fine-structure microscopy of organic and magnetic materials, Nat. Mater. 8 (4) (2009) 281–290, https://doi.org/10.1038/nmat2399.
[13] E.G. Rightor, A.P. Hitchcock, H. Ade, R.D. Leapman, S.G. Urquhart, A.P. Smith, G. Mitchell, D. Fischer, H.J. Shin, T. Warwick, Spectromicroscopy of poly (ethylene terephthalate): comparison of spectra and radiation damage rates in X-ray absorption and electron energy loss, J. Phys. Chem. B 101 (11) (1997) 1950–1960, https://doi.org/10.1021/jp9622748.
[14] J. van den Brand, O. Blajiev, P.C.J. Beentjes, H. Terryn, J.H.W. de Wit, Interaction of anhydride and carboxylic acid compounds with aluminum oxide surfaces studied using infrared reflection absorption spectroscopy, Langmuir 20 (15) (2004) 6308–6317, https://doi.org/10.1021/la0496845.
[15] Y.S. Chi, I.S. Choi, Reactivity control of carboxylic acid-terminated self-assembled monolayers on gold: acid fluoride versus interchain carboxylic anhydride, Langmuir 21 (25) (2005) 11765–11772, https://doi.org/10.1021/la050847e.
[16] H.J. Lee, A.C. Jamison, Y. Yuan, C. Li, S. Rittikulsittichai, I. Rusakova, T.R. Lee, Robust carboxylic acid-terminated organic thin films and nanoparticle protectants generated from bidentate alkanethiols, Langmuir 29 (33) (2013) 10432–10439, https://doi.org/10.1021/la4017118.
[17] R.G. Delaplane, J.A. Ibers, An X-ray study of α-oxalic acid dihydrate (COOH) 2.2 H2O and of its deuterium analogue,(COOD) 2.2 D2O: isotope effect in hydrogen bonding and anisotropic extinction effects, Acta Crystallogr. B: Struct. Sci. Cryst. 25 (12) (1969) 2423–2437, https://doi.org/10.1107/S0567740869005899.
[18] D.R. Baer, M.H. Engelhard, A.S. Lea, L.V. Saraf, Simple method for estimating and comparing x-ray damage rates, J. Vac. Sci. Technol. A 23 (6) (2005) 1740–1744, https://doi.org/10.1116/1.2073387.
[19] B.V. Crist, Handbook of monochromatic XPS spectra – polymers and polymers damaged by X-rays, John Wiley & Sons, Chichester, 2000.
[20] J. Wang, C. Morin, L. Li, A.P. Hitchcock, A. Scholl, A. Doran, Radiation damage in soft X-ray microscopy, J. Electron. Spectros. Relat. Phenomena. 170 (1–3) (2009) 25–36.
[21] D.R. Baer, G.E. McGuire, K. Artyushkova, C.D. Easton, M.H. Engelhard, A.G. Shard, Introduction to topical collection: reproducibility challenges and solutions with a focus on guides to XPS analysis, J. Vac. Sci. Technol. 39 (2) (2021), https://doi.org/10.1116/6.0000873.
[22] D.J. Morgan, S. Uthayasekaran, Revisiting degradation in the XPS analysis of polymers, Surf Interface Anal. 55 (6-7) (2023) 556–563, https://doi.org/10.1002/sia.7151.
[23] H. Sohrabpoor, M. Elyasi, M. Aldosari, N.E. Gorji, Modeling the PbI2 formation in perovskite solar cells using XRD/XPS patterns, Superlattices and Microstructures 97 (2016) 556–561, https://doi.org/10.1016/j.spmi.2016.07.026.
[24] T. Coffey, S.G. Urquhart, H. Ade, Characterization of the effects of soft X-ray irradiation on polymers, J. Electron Spectrosc. Relat. 122 (1) (2002) 65–78, https://doi.org/10.1016/S0368-2048(01)00342-5.
[25] D. Briggs, G. Beamson, Primary and secondary oxygen-induced C1s binding energy shifts in X-ray photoelectron spectroscopy of polymers, Anal. Chem. 64 (15) (1992) 1729–1736, https://doi.org/10.1021/ac00039a018.
[26] A.P. Ameen, R.J. Ward, R.D. Short, G. Beamson, D. Briggs, A high-resolution X-ray photoelectron spectroscopy study of trifluoroacetic anhydride labelling of hydroxyl groups: demonstration of the β shift due to -OC(O)CF3, Polymer 34 (9) (1993) 1795–1799, https://doi.org/10.1016/0032-3861(93)90418-A.
[27] S.R. Leadley, M.C. Davies, M. Vert, C. Braud, A.J. Paul, A.G. Shard, J.F. Watts, Probing the surface chemical structure of the novel biodegradable polymer poly (βmalic acid) and its ester derivatives using ToF-SIMS and XPS, Macromolecules 30 (22) (1997) 6920–6928, https://doi.org/10.1021/ma9702612.
[28] S.R. Leadley, J.F. Watts, The use of monochromated XPS to evaluate acid-base interactions at the PMMA/OXIDISED metal interface, J. Adhes. 60 (1-4) (1997) 175–196, https://doi.org/10.1080/00218469708014418.
[29] J.F. Watts, M.-L. Abel, C. Perruchot, C. Lowe, J.T. Maxted, R.G. White, Segregation and crosslinking in urea formaldehyde/epoxy resins: a study by highresolution XPS, J. Electron Spectrosc. Relat. 121 (1) (2001) 233–247, https://doi.org/10.1016/S0368-2048(01)00337-1.
[30] J. Eickmans, A. Otto, A. Goldmann, The transition from physisorbed to chemisorbed oxygen on silver films studied by photoemission, Surf. Sci. 149 (1) (1985) 293–312, https://doi.org/10.1016/S0039-6028(85)80029-7.
[31] F. A. Permatasari, A. H. Aimon, F. Iskandar, T. Ogi, K. Okuyama, Role of C–N Configurations in the Photoluminescence of Graphene Quantum Dots Synthesized by a Hydrothermal Route, Sci. Rep., 6. 1 21042 (2016) 1-8. https://doi.org/10.1038/srep21042.
[32] M. Feng, H. Petek, Y. Shi, H. Sun, J. Zhao, F. Calaza, M. Sterrer, H.-J. Freund, Cooperative chemisorption-induced physisorption of CO2 molecules by metal-organic chains, ACS Nano 9 (12) (2015) 12124–12136, https://doi.org/10.1021/acsnano.5b05222.
[33] G.P. Nayaka, Y. Zhang, P. Dong, D. Wang, Z. Zhou, J. Duan, X. Li, Y. Lin, Q. Meng, K.V. Pai, J. Manjanna, G. Santhosh, An environmental friendly attempt to recycle the spent li-ion battery cathode through organic acid leaching, J. Environ. Chem. Eng. 7 (1) (2019) 102854, https://doi.org/10.1016/j.jece.2018.102854.
[34] H.M. Ismail, D.A. Cadenhead, M.I. Zaki, Surface reactivity of iron oxide pigmentary powders toward atmospheric components: XPS, FESEM, and gravimetry of CO and CO2 adsorption, J. Colloid Interface Sci. 194 (2) (1997) 482–488, https://doi.org/10.1006/jcis.1997.5128.
[35] A.V. Shchukarev, D.V. Korolkov, XPS study of group IA carbonates, Open Chem. 2 (2) (2004) 347–362, https://doi.org/10.2478/BF02475578.
[36] A.R. Gonzalez-Elipe, J.P. Espinos, A. Fernandez, G. Munuera, XPS study of the surface carbonation/hydroxylation state of metal oxides, Appl. Surf. Sci. 45 (2) (1990) 103–108, https://doi.org/10.1016/0169-4332(90)90060-D.
[37] D.E. Fowler, C.R. Brundle, J. Lerczak, F. Holtzberg, Core and valence XPS spectra of clean, cleaved single crystals of YBa2Cu3O7, J. Electron Spectrosc. Relat. 52 (1990) 323–339, https://doi.org/10.1016/0368-2048(90)85029-9.
[38] J. Cruz-Castañeda, A. Negrón-Mendoza, D. Frías, M. Colín-García, A. Heredia, S. Ramos-Bernal, S. Villafañe-Barajas, Chemical evolution studies: the radiolysis and thermal decomposition of malonic acid, J. Radioanal. Nucl. Chem. 304 (1) (2015) 219–225, https://doi.org/10.1007/s10967-014-3711-z.
[39] K. Muraishi, Y. Suzuki, The thermal behaviour of dicarboxylic acids in various atmospheres, Thermochim. Acta. 232 (2) (1994) 195–203, https://doi.org/10.1016/0040-6031(94)80059-6.
[40] Y. Suzuki, K. Muraishi, K. Matsuki, Thermal behaviour of dicarboxylic acids. determination of melting points by DTA, Thermochim. Acta. 211 (1992) 171–180, https://doi.org/10.1016/0040-6031(92)87017-5.
[41] K. Muraishi, Y. Suzuki, A. Kikuchi, Kinetics of the thermal decomposition of dicarboxylic acids, Thermochim. Acta. 239 (1994) 51–59, https://doi.org/10.1016/0040-6031(94)87055-1.
[42] K. Clou, R. Keuleers, J. Janssens, H.O. Desseyn, Thermal behaviour of some dicarboxylic acids and their monoamide derivatives, Thermochim. Acta. 339 (1–2) (1999) 69–77, https://doi.org/10.1016/S0040-6031(99)00195-1.